FINITE ELEMENT MODELLING OF CRACKING IN FIBER-REINFORCED CONCRETE BEAMS

Carlos A. C. Brant[1], Gustavo. L. X. da Costa[1], Rodolfo G. M. de Andrade[2], Eduardo R. M. Fairbairn[1]
[1]*Civil Engineering Program, COPPE, Federal University of Rio de Janeiro*
Avenida Athos da Silveira Ramos, 149 –Centro de Tecnologia, Ilha do Fundão, Zip-Code 68506 - CEP 21941-909, Rio de Janeiro/Rio de Janeiro, Brazil
carlos.brant@coc.ufrj.br, gustavo.costa@coc.ufrj.br, eduardo@coc.ufrj.br
[2]*Engineering and Buildings Department, Federal Institute of Espírito Santo, Avenida Vitória, 29040-780, Espírito Santo, Brazil*
rodolfo.andrade@ifes.edu.br

Abstract. In this paper, a fiber-reinforced concrete beam is modelled in the framework of Finite Element Method. It is adopted three approaches, namely Smeared crack, Discrete crack and Damage models. The analyses are conducted through commercial software DIANA FEA and an in-house computational routine. To do so, it was selected an experimental data of concrete notched beam presented in literature to compare with the proposed models. First, Smeared crack model with Crackband regularization technique was studied and compared with Discrete crack model. The Discrete cracking approach was used to simulation and sought to reproduce the experimental Force-CMOD curve considering the experimental cracking pattern of the specimens. To do so, it was necessary to obtain mode I fracture energy (G_f), the tensile strength of the fiber-reinforced concrete (f_t) and the associated softening behavior. Numerical results show a convergence towards the experimental results. In parallel, the Damage models with crack band, nonlocal integral and interfaces elements techniques are also used to simulate the experimental structure. To do so, now it was necessary to obtain the maximum crack opening (w_u), f_t and the associated softening behavior. They demonstrate similar results when compared to laboratory tests.

Keywords: Concrete, Fiber-reinforced, Finite Element Method, Cracking.

1 Introduction

The phenomena of the pattern and propagation of cracks in concrete structures have been the object of study for at least five decades [1]. However, the choice of the method that best represents the reality of the cracking process in cementitious materials is still a matter of discussion among researchers [2]. For instance, the finite element program DIANA FEA allows two approaches to model the appearance and the propagation of cracks in concrete, namely Smeared cracking model and Discrete cracking model.

The Smeared cracking model imagines the cracked solid in terms of deformation in the continuous medium, i.e., the crack is fictitiously distributed in the continuous. This model allows a description in terms of stress and strain, and it can be directly implemented in the Finite Element Method (FEM) [3]. For this model, it is necessary to introduce the concept of Crackband (l_b), which is a characteristic length where the crack will be distributed. For Rots [4], l_b depends on the size, shape and interpolation function used in the finite element. For two-dimensional linear elements $l_b = \sqrt{2A}$ and for two-dimensional elements of higher orders $l_b = \sqrt{A}$, where A is the area of the finite element. For solid elements $l_b = \sqrt{V}$, where V is the volume of the finite element.

On the other hand, the Discrete cracking model represents the cracking phenomenon more closely, as it uses interface elements where the crack can form and propagate. Thus, the development of the crack is parallel to the geometric discontinuity that separates the material into parts. [3]. Unlike the Smeared cracking model, this model is described in terms of stress and crack opening in the post-peak diagram.

Also in this work, damage models are used. For that, a scalar and isotropic damage model is adopted, applying the crack band and non-local integral type techniques, demonstrating parallel results and experimental tests. The analyzes led to some results in terms of the Force- crack mouth opening displacement (CMOD) curve despite the cracking pattern, especially when dealing with fiber reinforced structures that present very tortuous and irregular cracks. To circumvent this issue, one will resort to Discrete models by means of interface elements. Interface elements are placed between all continuum elements to allow the structure to develop cracks wherever necessary. This will lead to meaningful crack paths although they do not exactly match with experimental observations. Thus, it is conducted a retro-analysis where a biased mesh is generated for which crack planes coincide with those observed in photograph.

So, this paper aims to consider Discrete cracking model and Damage models with crack band, nonlocal integral and interfaces elements techniques to analyze a steel fiber-reinforced concrete beam tested by Andrade [5]. A description of the steps is presented in the next sections.

1.1 Smeared cracking model in a concrete beam subjected to bending moment at three points

In this section, a model of a fiber-reinforced concrete beam subjected to three point bending test (see Figure 1) is carried out using DIANA FEA program. Here, the pattern and propagation of the crack will be modeled according to the Smeared crack model.

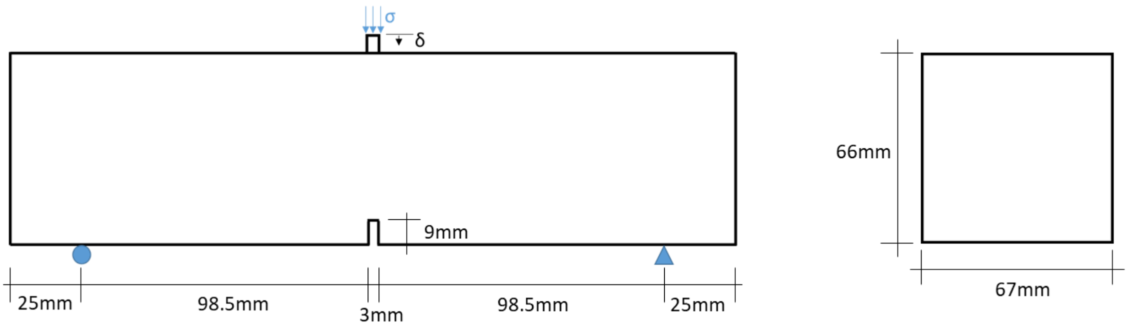

Figure 1. Three point bending test setup and beam dimensions (CP9 6x6x25)

In Figure 2, the mesh used for the analysis can be seen. In the central section of interest, there are 3x3 mm² quadrilateral elements with quadratic interpolation function ($l_b = \sqrt{9} = 3$mm). As shown in Figure 2, the outer parts of the model were considered to behave elastically, while the inner part, nonlinearly (Smeared crack). The Modulus of Elasticity of the concrete beam was equal to 30 GPa, and a tensile strength of 4,5 MPa was adopted for the inner part.

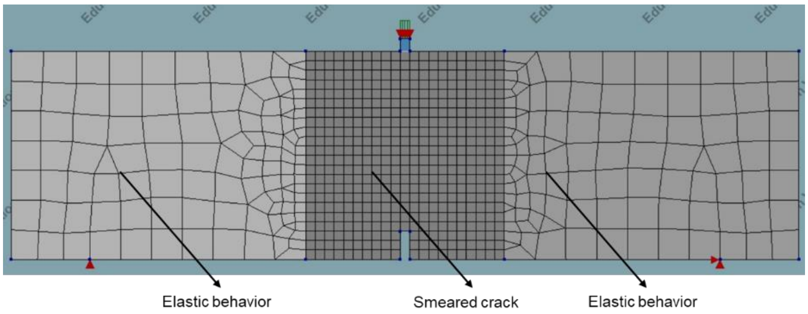

Figure 2. Mesh and analysis sections, Smeared cracking model

The stress-strain diagrams considered for the central part is presented in Figure 3. In this figure, it can be seen the maximum elastic strain $\varepsilon_{e,lim}$ = 0.00015 and the maximum crack opening at w_u = 4.5 mm.

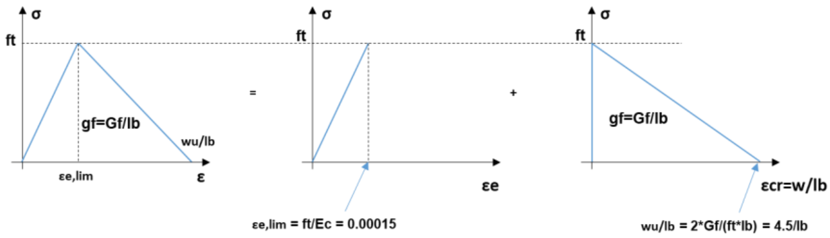

Figure 3. Linear behavior of tensile stress and strain of Smeared cracking model

From the simulation outputs, a force- CMOD curve, and the crack pattern are shown in Figures 4.

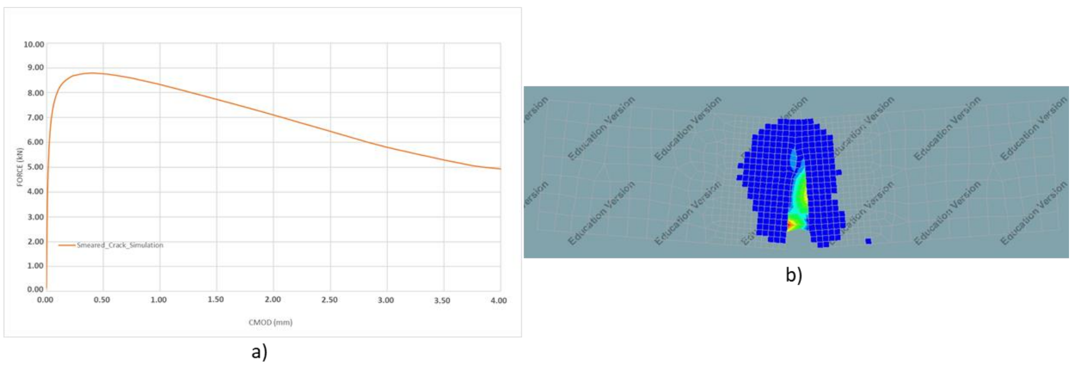

Figure 4. a) Force-CMOD curve, Smeared cracking model; b) Smeared crack pattern in the last load step

In Figure 4.b, the occurrence of many small nucleated cracks that connect at a more advanced loading stage and form a dominant crack can be seen, as already noted by De Borst, et al. [2].

1.2 Discrete cracking model in a concrete beam subjected to bending moment at three points

In this step, the same approach that what was done in the previous section is repeated, but considering the Discrete cracking model.

Figure 5.a shows the mesh used for the analysis, with the central part of interest presenting quadrilateral

elements with 1.5 x 1.5 mm dimensions and with quadratic interpolation function ($l_b = \sqrt{2.25} = 1.5$mm). Only a single vertical interface line where the crack can develop in Discrete cracking model was considered. All area elements behave elastically with the same Modulus of Elasticity adopted in section 1.1, as well as the single interface line's tensile strength.

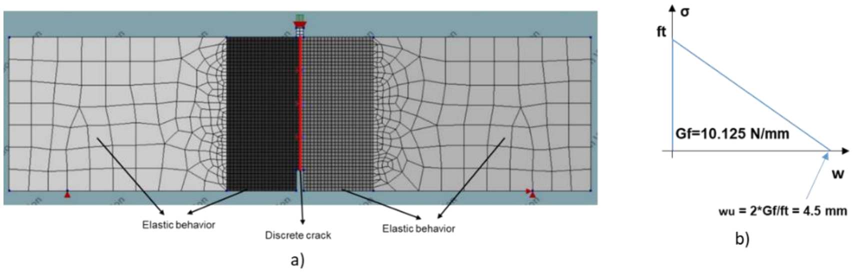

Figure 5. a) Mesh and analysis sections, Discrete cracking model; b) Linear softening behavior of tensile stress and crack opening displacement of Discrete crack model

For the interface element, the tensile stress crack opening diagram is shown in Figure 5.b. It is possible to verify the crack energy for mode 1 Gf = 10.125 N/mm and the maximum crack opening $w_u = 4.5$ mm.

From the simulation outputs, a force-CMOD curve and the cracking pattern are shown in Figures 6.

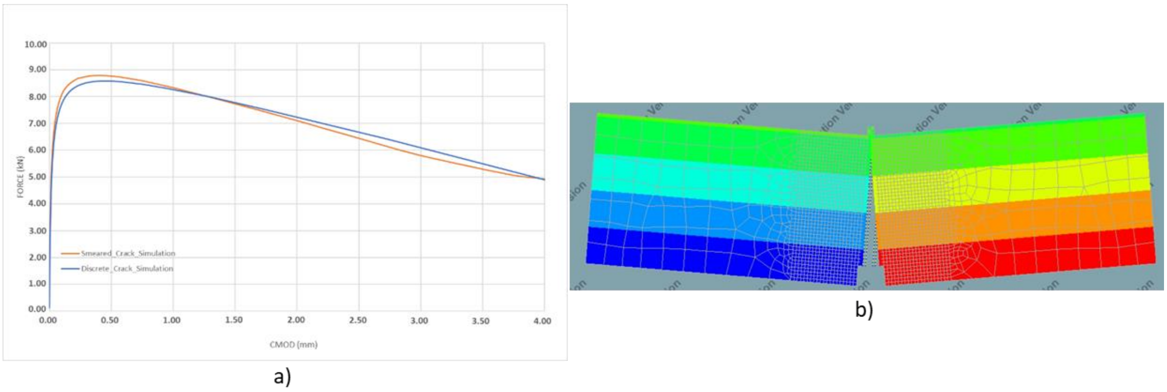

Figure 6. a) Force-CMOD curve, Discrete crack model, compared with Smeared crack model; b) Discrete crack pattern in the last loading step

In Figure 6.a, similar results between Smeared and Discrete crack models were observed. In the development of the crack pattern (Figure 6.b), a direct occurrence of a single crack can be seen, as already noted by De Borst, et al. [2] when referring to discrete crack.

In this sense, it was decided the Discrete Crack Model is more convenient to use when modelling an experimentally predefined cracking pattern. Thus, this approach and Damage models with crack band, nonlocal integral and interfaces elements techniques are used in Section 2.

2 Experimental validation

In this section, a comparison among the numerical models and the experimental result is presented. The experimental result was obtained from the Andrade [5], with a fiber-reinforced concrete beam (CP9 6x6x25) tested under three point bending tests. For the numerical analyses, the Discrete crack and the Damage models were used.

2.1 Analysis of CP9 6x6x25

The geometry of the CP9 beam is shown in Figure 1, and Figure 7.a shows its Force-Deflection experimental curve. To help finding Gf value (given in Equation 1), an extrapolation curve was used; a linear softening curve was found to be representative for the sake of this work.

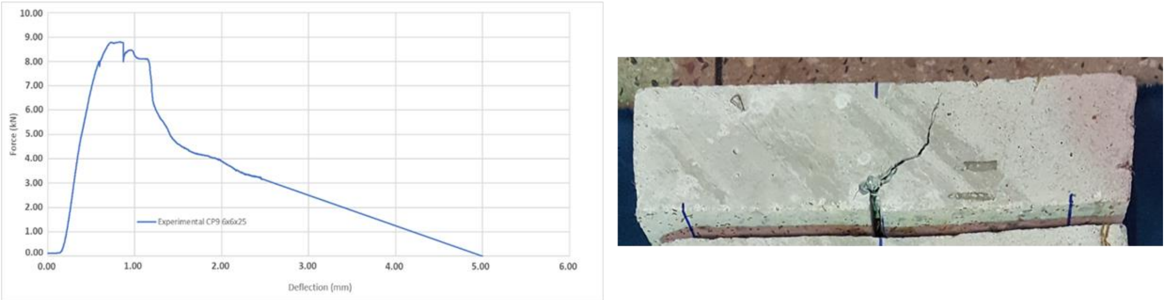

Figure 7. a) Behavior Px$\boldsymbol{\delta}$ of CP9 6x6x25; b) Real cracking pattern CP9 6x6x25, font [5]

$$\text{Gf} = \int Pd\delta\,/A_{crack} = 316355.67/A_{crack}\ \text{[N/mm]} \quad (1)$$

Where P is the force imposed by the hydraulic press and A_{crack} is the area of the crack surface.

It is recommended that the area of the crack surface is compared with a computer tomography of the beam after the test. The cracking pattern on one side of the CP9 was registered in Figure 7.b.

Analysis with the Discrete crack model

For this numerical model approach, Gf value was calculated in accordance with Equation 1. The ft values were related with the angle of the crack and a shape of linear softening.

Before running the model, discrete elements (Figure 8.a) were inserted as pre-cracks so the crack could propagate in a similar fashion as the experimental cracking pattern registered in Figure 7.b.

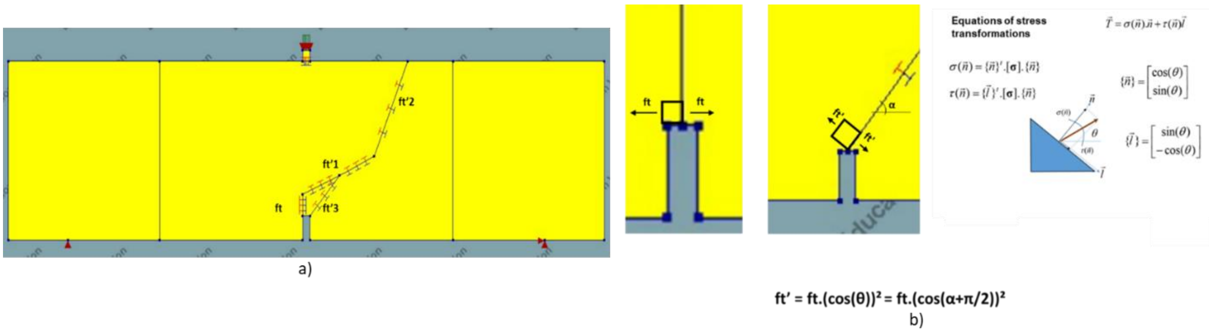

Figure 8. a) Simulation of the cracking pattern CP9 6x6x25; b) Transformation of tensile stress ft into ft'

It is understood that the crack tends to propagate on the path where the tensile stresses are highest. Thus, the change in the direction of the crack was associated with the penalty of the tensile strength, as shown in Figure 8.b.

It is assumed that if the tensile strength in the crack plane is less than ft', the crack should open in that location. This may be due to the arrangement of the steel fibers, which were perpendicularly positioned to the direction of the principal tensile stress. In other words, it is assumed that the orientation of the fibers can make the behavior of the fiber-reinforced concrete orthotropic.

So, for this example, A_{crack} = 6488.96 mm², G_f = 2.52 N/mm, and f_t = 3.2 MPa, $f_{t'1}$ = 0.62 MPa, $f_{t'2}$ = 2.76 MPa and $f_{t'3}$ = 1.88 MPa. Furthermore, the modulus of elasticity of the concrete was E_c = 30GPa.

The results of the simulation and experimental are shown in Figure 9.a. The associated cracking pattern is shown in Figure 9.b, below.

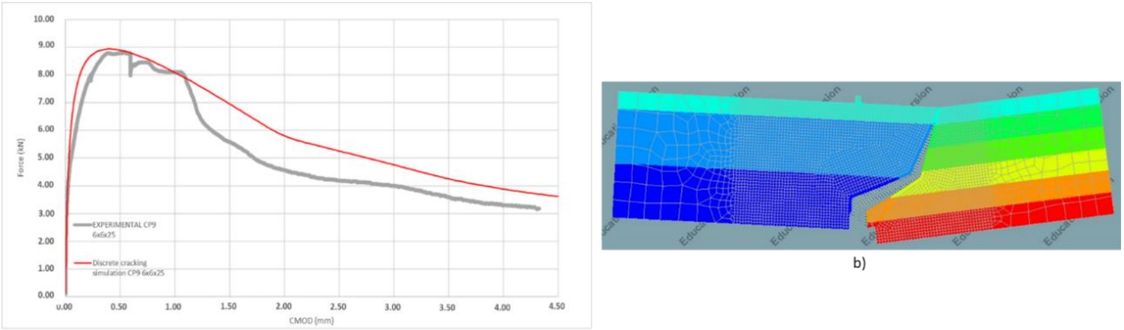

a) b)

Figure 9. a) Results of imposed force by CMOD; b) Discrete crack pattern in the last loading step (CP9 6x6x25)

Analysis with the Damage models

Three simulations were carried out employing the following cracking models: scalar isotropic damage with Crack band, scalar isotropic damage with Nonlocal integral and Cohesive Zone with Interfaces Elements. For more details about these models the interested reader is referred to the companion paper by Costa *et al.* [6]. Input data for simulations are in Table 1. The simulations and experimental results as well as the cracking patterns are in Figure 10.

The Force-CMOD curves agree quite well with the laboratory test, but the crack pattern doesn't. The simulations don't display the highly tortuous and irregular crack pattern of experiments in fiber-reinforced concrete structures. This is because concrete and fiber are considered as a single homogeneous material so the present model doesn't differ too much from a plain concrete model except for its high Fracture Energy.

Table 1. Input parameters for simulations with Damage models

	Crackband	Nonlocal integral	Discrete
f_t (MPa)	5.20	4.00	4.90
w_u (mm)	8.00	--	7.00
Characteristic length – l_b	$\sqrt{A}$	5.00 mm	--
ε_f	w_u/l_b	1.50	--
Softening-type	Hordijk	Hordijk	Hordijk
Crack criterion	Rankine	Rankine	Rankine
E (GPa)	20.00	20.00	20.00
$E_{interface}$ ($N.mm^{-3}$)	--	--	10^6
Poisson ratio	0.20	0.20	0.20
Weighting function	--	Quartic polynomial	--

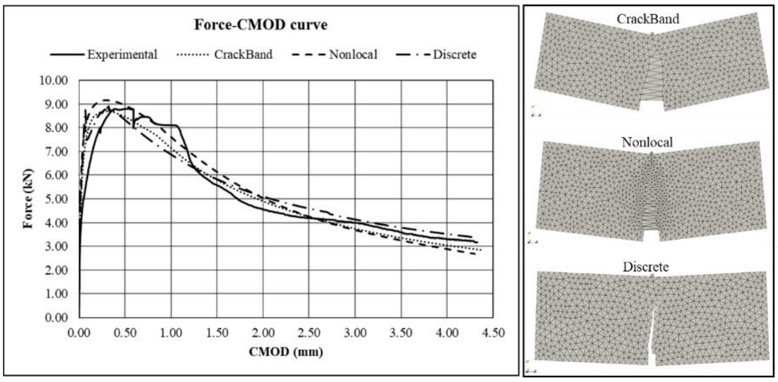

a) b)

Figure 10. a) Damage model results of imposed force by CMOD for CP9 6x6x25; b) Cracking patterns

3 Conclusions

In this paper, a fiber-reinforced concrete beam was modelled in the framework of Finite Element Method. It was adopted three approaches, namely Smeared crack, Discrete crack, and Damage models to simulate a fiber-reinforced concrete notched beam presented in literature.

Two basic results could be extracted from the simulations, the behavior of the Force-CMOD curve and the cracking pattern in the last load step. From Figures 9.a and 10.a all the graphs obtained in the simulations tend to reproduce the expected experimental behavior. On the other hand, the cracking pattern was closer with the simulations using Discrete cracking (Figure 9.b) and Damage model with interface elements (Figure 10.b; last figure). The first is associated with the imposition of the planes where the crack will occur and the second is random, depending essentially on the tensile strength and the shape of the mesh.

On the other hand, the Damage models used input parameters more freely while the discrete cracking model sought to stick to the experimental parameters, mainly regarding the calculation of G_f.

Regarding the computational cost, Damage models require more time than the Discrete cracking model, especially the Damage model with the interface elements technique.

Finally, it is emphasized that trying to represent the mechanical behavior of a fiber-reinforced concrete beam is not trivial, especially when considering the homogeneous material. This shows that replacing the effects of direction, concentration, and adhesion of fibers in concrete by given compensations of G_f, f_t and softening shape requires a lot of care in practice.

Acknowledgements. This study was financed in part by the Brazilian Agency Coordenação de Aperfeiçoamento de Pessoal de Nível Superior (CAPES) —Finance Code 001. The support of Brazilian funding agencies Conselho Nacional de Desenvolvimento Científico e Tecnológico (CNPq) and Fundação de Amparo à Pesquisa do Estado do Rio de Janeiro (FAPERJ) are also gratefully acknowledged.

Authorship statement. The authors hereby confirm that they are the sole liable persons responsible for the authorship of this work, and that all material that has been herein included as part of the present paper is either the property (and authorship) of the authors or has the permission of the owners to be included here.

References

[1] J. G. Rots; P. Nauta; G. M. A. Kusters; J. Blaauwendraad. Smeared Crack Approach and Fracture Localization in Concrete, v. 30, n. 1, 1985.
[2] R. De Borst; J. J. C. Remmers; A. Needleman; M. A. Abellan. Discrete vs smeared crack models for concrete fracture: bridging the gap. International Journal for Numerical and Analytical Methods in Geomechanics, v. 28, p. 583-607, 2004.
[3] J. G. Rots and J. Blaauwendraad. Crack Models for Concrete: Discrete or Smeared? Fixed, Multi-Directional or Rotating? Heron, v. 34, n. 1, 1989.
[4] J. G. Rots. Computational Modeling of Concrete Fracture. PhD thesis, Delft University of Technology, 1988.
[5] R. G. Mendes de Andrade. Estrutura Pré-Fabricada de Concreto de Alto Desempenho Reforçado com Fibras de Aço para Pontilhões Rodoviários. Tese de Doutorado, PEC/COPPE/UFRJ. Rio de Janeiro, 2020.
[6] G. L. X. da Costa, C. A. C. Brant, R. G. M. de Andrade, E. M. R. Fairbairn. Finite Element Analyses of mesh-objectivity for Smeared, Damage and Discrete models applied to concrete cracking. Artigo aceito em congresso: XLII CILAMCE/ III PANACM. Rio de Janeiro. 2021.